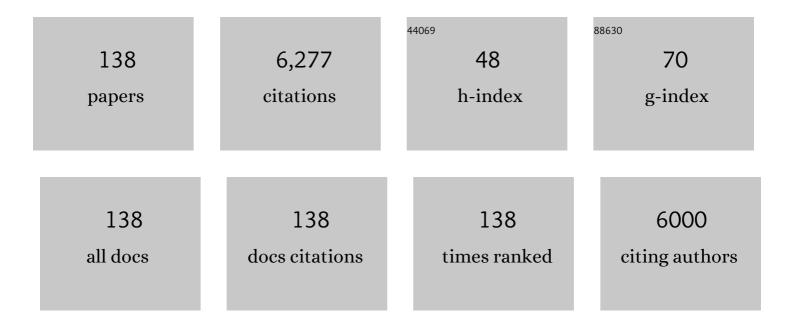
List of Publications by Year in descending order

Source: https://exaly.com/author-pdf/6995566/publications.pdf Version: 2024-02-01



#	Article	IF	CITATIONS
1	Design and fabrication of effective gradient temperature sensor array based on bilayer SnO2/Pt for gas classification. Sensors and Actuators B: Chemical, 2022, 351, 130979.	7.8	11
2	Investigation of zinc electronucleation and growth mechanisms onto platinum electrode from a deep eutectic solvent for gas sensing applications. Journal of Applied Electrochemistry, 2022, 52, 299-309.	2.9	8
3	Low-operating temperature and remarkably responsive methanol sensors using Pt-decorated hierarchical ZnO structure. Nanotechnology, 2022, 33, 065502.	2.6	3
4	Superior detection and classification of ethanol and acetone using 3D ultra-porous Î ³ -Fe2O3 nanocubes-based sensor. Sensors and Actuators B: Chemical, 2022, 362, 131737.	7.8	11
5	A novel design and fabrication of self-heated In2O3 nanowire gas sensor on glass for ethanol detection. Sensors and Actuators A: Physical, 2022, 345, 113769.	4.1	24
6	Au doped ZnO/SnO2 composite nanofibers for enhanced H2S gas sensing performance. Sensors and Actuators A: Physical, 2021, 317, 112454.	4.1	30
7	Highly selective H2S gas sensor based on WO3-coated SnO2 nanowires. Materials Today Communications, 2021, 26, 102094.	1.9	29
8	Comparative study on the gas-sensing performance of ZnO/SnO2 external and ZnO–SnO2 internal heterojunctions for ppb H2S and NO2 gases detection. Sensors and Actuators B: Chemical, 2021, 334, 129606.	7.8	65
9	Enhanced NH3 and H2 gas sensing with H2S gas interference using multilayer SnO2/Pt/WO3 nanofilms. Journal of Hazardous Materials, 2021, 412, 125181.	12.4	52
10	MoS2 nanosheets-decorated SnO2 nanofibers for enhanced SO2 gas sensing performance and classification of CO, NH3 and H2 gases. Analytica Chimica Acta, 2021, 1167, 338576.	5.4	29
11	Significantly enhanced NO2 gas-sensing performance of nanojunction-networked SnO2 nanowires by pulsed UV-radiation. Sensors and Actuators A: Physical, 2021, 327, 112759.	4.1	31
12	Enhanced NO2 gas-sensing performance at room temperature using exfoliated MoS2 nanosheets. Sensors and Actuators A: Physical, 2021, 332, 113137.	4.1	28
13	Extraordinary H2S gas sensing performance of ZnO/rGO external and internal heterojunctions. Journal of Alloys and Compounds, 2021, 879, 160457.	5.5	23
14	Room temperature highly toxic NO2 gas sensors based on rootstock/scion nanowires of SnO2/ZnO, ZnO/SnO2, SnO2/SnO2 and, ZnO/ZnO. Sensors and Actuators B: Chemical, 2021, 348, 130652.	7.8	40
15	One-step fabrication of SnO2 porous nanofiber gas sensors for sub-ppm H2S detection. Sensors and Actuators A: Physical, 2020, 303, 111722.	4.1	98
16	VOC gas sensor based on hollow cubic assembled nanocrystal Zn2SnO4 for breath analysis. Sensors and Actuators A: Physical, 2020, 302, 111834.	4.1	50
17	Effective monitoring and classification of hydrogen and ammonia gases with a bilayer Pt/SnO2 thin film sensor. International Journal of Hydrogen Energy, 2020, 45, 2418-2428.	7.1	51
18	Dip-coating decoration of Ag ₂ O nanoparticles on SnO ₂ nanowires for high-performance H ₂ S gas sensors. RSC Advances, 2020, 10, 17713-17723.	3.6	17

#	Article	IF	CITATIONS
19	Prototype edge-grown nanowire sensor array for the real-time monitoring and classification of multiple gases. Journal of Science: Advanced Materials and Devices, 2020, 5, 409-416.	3.1	15
20	Enhanced H2S gas-sensing performance of α-Fe2O3 nanofibers by optimizing process conditions and loading with reduced graphene oxide. Journal of Alloys and Compounds, 2020, 826, 154169.	5.5	26
21	Nanoporous NiO nanosheets-based nanohybrid catalyst for efficient reduction of triiodide ions. Solar Energy, 2020, 197, 546-552.	6.1	17
22	Facile synthesis of ultrafine rGO/WO3 nanowire nanocomposites for highly sensitive toxic NH3 gas sensors. Materials Research Bulletin, 2020, 125, 110810.	5.2	80
23	Realization of a portable H2S sensing instrument based on SnO2 nanowires. Journal of Science: Advanced Materials and Devices, 2020, 5, 40-47.	3.1	9
24	Controlled Growth of Vertically Oriented Trilayer MoS ₂ Nanoflakes for Roomâ€Temperature NO ₂ Gas Sensor Applications. Physica Status Solidi (A) Applications and Materials Science, 2020, 217, 2000004.	1.8	16
25	Controlled synthesis of ultrathin MoS ₂ nanoflowers for highly enhanced NO ₂ sensing at room temperature. RSC Advances, 2020, 10, 12759-12771.	3.6	67
26	Facile post-synthesis and gas sensing properties of highly porous NiO microspheres. Sensors and Actuators A: Physical, 2019, 296, 110-120.	4.1	40
27	Facile Hydrothermal Synthesis of Two-Dimensional Porous ZnO Nanosheets for Highly Sensitive Ethanol Sensor. Journal of Nanomaterials, 2019, 2019, 1-7.	2.7	13
28	Facile and Scalable Fabrication of Highly Porous Co3O4 and α-Fe2O3 Nanosheets and Their Catalytic Properties. Journal of Electronic Materials, 2019, 48, 7897-7905.	2.2	1
29	A facile synthesis of ruthenium/reduced graphene oxide nanocomposite for effective electrochemical applications. Solar Energy, 2019, 191, 420-426.	6.1	21
30	Effective design and fabrication of low-power-consumption self-heated SnO2 nanowire sensors for reducing gases. Sensors and Actuators B: Chemical, 2019, 295, 144-152.	7.8	35
31	An effective H ₂ S sensor based on SnO ₂ nanowires decorated with NiO nanoparticles by electron beam evaporation. RSC Advances, 2019, 9, 13887-13895.	3.6	26
32	New Design of ZnO Nanorod- and Nanowire-Based NO ₂ Room-Temperature Sensors Prepared by Hydrothermal Method. Journal of Nanomaterials, 2019, 2019, 1-9.	2.7	17
33	Konjac glucomannan-templated synthesis of three-dimensional NiO nanostructures assembled from porous NiO nanoplates for gas sensors. RSC Advances, 2019, 9, 9584-9593.	3.6	21
34	Self-heated Ag-decorated SnO2 nanowires with low power consumption used as a predictive virtual multisensor for H2S-selective sensing. Analytica Chimica Acta, 2019, 1069, 108-116.	5.4	37
35	Transition metal oxides as Pt-free counter electrodes for liquid-junction photovoltaic devices. Vietnam Journal of Chemistry, 2019, 57, 784-791.	0.8	9
36	Magnetic iron oxide nanoparticles decorated graphene for chemoresistive gas sensing: The particle size effects. Journal of Colloid and Interface Science, 2019, 539, 315-325.	9.4	37

#	Article	IF	CITATIONS
37	Excellent detection of H2S gas at ppb concentrations using ZnFe2O4 nanofibers loaded with reduced graphene oxide. Sensors and Actuators B: Chemical, 2019, 282, 876-884.	7.8	75
38	Urea mediated synthesis of Ni(OH) 2 nanowires and their conversion into NiO nanostructure for hydrogen gas-sensing application. International Journal of Hydrogen Energy, 2018, 43, 9446-9453.	7.1	46
39	Ultrasensitive NO2 gas sensors using hybrid heterojunctions of multi-walled carbon nanotubes and on-chip grown SnO2 nanowires. Applied Physics Letters, 2018, 112, .	3.3	26
40	C ₂ H ₅ OH and NO ₂ sensing properties of ZnO nanostructures: correlation between crystal size, defect level and sensing performance. RSC Advances, 2018, 8, 5629-5639.	3.6	55
41	Comparison of NO2 Gas-Sensing Properties of Three Different ZnO Nanostructures Synthesized by On-Chip Low-Temperature Hydrothermal Growth. Journal of Electronic Materials, 2018, 47, 785-793.	2.2	18
42	Mesoporous Cobalt Tungsten Oxide Heterostructured Nanotoroids for Gas Sensing. Advanced Materials Interfaces, 2018, 5, 1800269.	3.7	6
43	Fe2O3 nanoporous network fabricated from Fe3O4/reduced graphene oxide for high-performance ethanol gas sensor. Sensors and Actuators B: Chemical, 2018, 255, 3275-3283.	7.8	120
44	Controlled synthesis of manganese tungstate nanorods for highly selective NH3 gas sensor. Journal of Alloys and Compounds, 2018, 735, 787-794.	5.5	41
45	Ultralow power consumption gas sensor based on a self-heated nanojunction of SnO ₂ nanowires. RSC Advances, 2018, 8, 36323-36330.	3.6	23
46	SO2 and H2S Sensing Properties of Hydrothermally Synthesized CuO Nanoplates. Journal of Electronic Materials, 2018, 47, 7170-7178.	2.2	27
47	A comparative study on the electrochemical properties of nanoporous nickel oxide nanowires and nanosheets prepared by a hydrothermal method. RSC Advances, 2018, 8, 19449-19455.	3.6	57
48	Nanoporous and crystal evolution in nickel oxide nanosheets for enhanced gas-sensing performance. Sensors and Actuators B: Chemical, 2018, 273, 784-793.	7.8	47
49	Facile on-chip electrospinning of ZnFe2O4 nanofiber sensors with excellent sensing performance to H2S down ppb level. Journal of Hazardous Materials, 2018, 360, 6-16.	12.4	87
50	Simple post-synthesis of mesoporous p-type Co3O4 nanochains for enhanced H2S gas sensing performance. Sensors and Actuators B: Chemical, 2018, 270, 158-166.	7.8	53
51	Selective discrimination of hazardous gases using one single metal oxide resistive sensor. Sensors and Actuators B: Chemical, 2018, 277, 121-128.	7.8	54
52	Comparative effects of synthesis parameters on the NO2 gas-sensing performance of on-chip grown ZnO and Zn2SnO4 nanowire sensors. Journal of Alloys and Compounds, 2018, 765, 1237-1242.	5.5	32
53	Novel Self-Heated Gas Sensors Using on-Chip Networked Nanowires with Ultralow Power Consumption. ACS Applied Materials & amp; Interfaces, 2017, 9, 6153-6162.	8.0	53
54	On-chip growth of single phase Zn2SnO4 nanowires by thermal evaporation method for gas sensor application. Journal of Alloys and Compounds, 2017, 708, 470-475.	5.5	23

NGUYEN VAN HIEU

#	Article	IF	CITATIONS
55	Elaboration of Pd-nanoparticle decorated polyaniline films for room temperature NH3 gas sensors. Sensors and Actuators B: Chemical, 2017, 249, 348-356.	7.8	75
56	On-chip growth of patterned ZnO nanorod sensors with PdO decoration for enhancement of hydrogen-sensing performance. International Journal of Hydrogen Energy, 2017, 42, 16294-16304.	7.1	34
57	Bilayer SnO2–WO3 nanofilms for enhanced NH3 gas sensing performance. Materials Science and Engineering B: Solid-State Materials for Advanced Technology, 2017, 224, 163-170.	3.5	67
58	On-chip growth of semiconductor metal oxide nanowires for gas sensors: A review. Journal of Science: Advanced Materials and Devices, 2017, 2, 263-285.	3.1	84
59	Superior enhancement of NO2 gas response using n-p-n transition of carbon nanotubes/SnO2 nanowires heterojunctions. Sensors and Actuators B: Chemical, 2017, 238, 1120-1127.	7.8	53
60	CuO Nanofibers Prepared by Electrospinning for Gas Sensing Application: Effect of Copper Salt Concentration. Journal of Nanoscience and Nanotechnology, 2016, 16, 7910-7918.	0.9	11
61	Synthesis and gas-sensing characteristics of α-Fe2O3 hollow balls. Journal of Science: Advanced Materials and Devices, 2016, 1, 45-50.	3.1	37
62	On-chip hydrothermal growth of ZnO nanorods at low temperature for highly selective NO2 gas sensor. Materials Letters, 2016, 169, 231-235.	2.6	50
63	Chlorine Gas Sensing Performance of On-Chip Grown ZnO, WO ₃ , and SnO ₂ Nanowire Sensors. ACS Applied Materials & Interfaces, 2016, 8, 4828-4837.	8.0	116
64	Ultrasensitive NO2 gas sensors using tungsten oxide nanowires with multiple junctions self-assembled on discrete catalyst islands via on-chip fabrication. Sensors and Actuators B: Chemical, 2016, 227, 198-203.	7.8	27
65	Nitrogen-Doped Graphene Synthesized from a Single Liquid Precursor for a Field Effect Transistor. Journal of Electronic Materials, 2016, 45, 839-845.	2.2	12
66	Enhancement of gas-sensing characteristics of hydrothermally synthesized WO3 nanorods by surface decoration with Pd nanoparticles. Sensors and Actuators B: Chemical, 2016, 223, 453-460.	7.8	70
67	Fabrication of highly sensitive and selective H2 gas sensor based on SnO2 thin film sensitized with microsized Pd islands. Journal of Hazardous Materials, 2016, 301, 433-442.	12.4	119
68	Ammonia-Gas-Sensing Characteristics of WO ₃ /Carbon Nanotubes Nanocomposites: Effect of Nanotube Content and Sensing Mechanism. Science of Advanced Materials, 2016, 8, 524-533.	0.7	15
69	The Dependence of a Quantum Acoustoelectric Current on Some Qualities in a Cylindrical Quantum Wire with an Infinite Potential GaAs/GaAsAl. Materials Transactions, 2015, 56, 1408-1411.	1.2	5
70	Meso-/Nanoporous Semiconducting Metal Oxides for Gas Sensor Applications. Journal of Nanomaterials, 2015, 2015, 1-14.	2.7	71
71	lsotropic metamaterial absorber using cut-wire-pair structures. Applied Physics Express, 2015, 8, 032001.	2.4	17
72	Micro-wheels composed of self-assembled tungsten oxide nanorods for highly sensitive detection of low level toxic chlorine gas. RSC Advances, 2015, 5, 25204-25207.	3.6	27

#	Article	IF	CITATIONS
73	Shape and size controlled synthesis of Au nanorods: H 2 S gas-sensing characterizations and antibacterial application. Journal of Alloys and Compounds, 2015, 635, 265-271.	5.5	29
74	Effects of gamma irradiation on hydrogen gas-sensing characteristics of Pd–SnO2 thin filmÂsensors. International Journal of Hydrogen Energy, 2015, 40, 12572-12580.	7.1	54
75	Facile synthesis of α-Fe 2 O 3 nanoparticles for high-performance CO gas sensor. Materials Research Bulletin, 2015, 68, 302-307.	5.2	80
76	Synthesis, characterization, and comparative gas sensing properties of tin dioxide nanoflowers and porous nanospheres. Ceramics International, 2015, 41, 14819-14825.	4.8	19
77	Taming electromagnetic metamaterials for isotropic perfect absorbers. AIP Advances, 2015, 5, .	1.3	7
78	Facile synthesis of single-crystal nanoporous α-NiS nanosheets from Ni(OH)2 counterpart. Materials Letters, 2015, 161, 282-285.	2.6	10
79	Scalable fabrication of SnO2 thin films sensitized with CuO islands for enhanced H2S gas sensing performance. Applied Surface Science, 2015, 324, 280-285.	6.1	34
80	Outstanding gas-sensing performance of graphene/SnO2 nanowire Schottky junctions. Applied Physics Letters, 2014, 105, .	3.3	93
81	Full-Layer Controlled Synthesis and Transfer of Large-Scale Monolayer Graphene for Nitrogen Dioxide and Ammonia Sensing. Analytical Letters, 2014, 47, 280-294.	1.8	15
82	Controllable growth of ZnO nanowires grown on discrete islands of Au catalyst for realization of planar-type micro gas sensors. Sensors and Actuators B: Chemical, 2014, 193, 888-894.	7.8	69
83	Facile preparation of large-scale α-Fe2O3 nanorod/SnO2 nanorod composites and their LPG-sensing properties. Journal of Alloys and Compounds, 2014, 599, 195-201.	5.5	19
84	Effective decoration of Pd nanoparticles on the surface of SnO2 nanowires for enhancement of CO gas-sensing performance. Journal of Hazardous Materials, 2014, 265, 124-132.	12.4	125
85	Single crystal cupric oxide nanowires: Length- and density-controlled growth and gas-sensing characteristics. Physica E: Low-Dimensional Systems and Nanostructures, 2014, 58, 16-23.	2.7	8
86	Novel portable electrical detection system for DNA SENSOR application. Journal of Experimental Nanoscience, 2014, 9, 652-660.	2.4	1
87	Scalable Fabrication of High-Performance NO ₂ Gas Sensors Based on Tungsten Oxide Nanowires by On-Chip Growth and RuO ₂ -Functionalization. ACS Applied Materials & Interfaces, 2014, 6, 12022-12030.	8.0	36
88	Nanoporous hematite nanoparticles: Synthesis and applications for benzylation of benzene and aromatic compounds. Journal of Alloys and Compounds, 2014, 582, 83-87.	5.5	21
89	Comparative NO2 gas-sensing performance of the self-heated individual, multiple and networked SnO2 nanowire sensors fabricated by a simple process. Sensors and Actuators B: Chemical, 2014, 201, 7-12.	7.8	51
90	Tungsten Oxide Urchin-Flowers and Nanobundles: Effect of Synthesis Conditions and Heat Treatment on Assembly and Gas-Sensing Characteristics. Science of Advanced Materials, 2014, 6, 1081-1090.	0.7	6

#	Article	IF	CITATIONS
91	Density-controllable growth of SnO2 nanowire junction-bridging across electrode for low-temperature NO2 gas detection. Journal of Materials Science, 2013, 48, 7253-7259.	3.7	21
92	In-situ decoration of Pd nanocrystals on crystalline mesoporous NiO nanosheets for effective hydrogen gas sensors. International Journal of Hydrogen Energy, 2013, 38, 12090-12100.	7.1	61
93	General and scalable route to synthesize nanowire-structured semiconducting metal oxides for gas-sensor applications. Journal of Alloys and Compounds, 2013, 549, 260-268.	5.5	32
94	Facile synthesis of SnO2–ZnO core–shell nanowires for enhanced ethanol-sensing performance. Current Applied Physics, 2013, 13, 1637-1642.	2.4	53
95	The quantum acoustoelectric current in a doped superlattice GaAs:Si/GaAs:Be. Superlattices and Microstructures, 2013, 63, 121-130.	3.1	8
96	Comparative study on CO2 and CO sensing performance of LaOCl-coated ZnO nanowires. Journal of Hazardous Materials, 2013, 244-245, 209-216.	12.4	51
97	Single-crystal zinc oxide nanorods with nanovoids as highly sensitive NO2 nanosensors. Materials Letters, 2013, 94, 41-43.	2.6	21
98	On-chip growth of wafer-scale planar-type ZnO nanorod sensors for effective detection of CO gas. Sensors and Actuators B: Chemical, 2013, 181, 529-536.	7.8	74
99	Diameter controlled synthesis of tungsten oxide nanorod bundles for highly sensitive NO2 gas sensors. Sensors and Actuators B: Chemical, 2013, 183, 372-380.	7.8	70
100	Polyaniline Nanowires-Based Electrochemical Immunosensor for Label Free Detection of Japanese Encephalitis Virus. Analytical Letters, 2013, 46, 1229-1240.	1.8	26
101	Crystalline mesoporous tungsten oxide nanoplate monoliths synthesized by directed soft template method for highly sensitive NO2 gas sensor applications. Materials Research Bulletin, 2013, 48, 440-448.	5.2	39
102	Selective detection of carbon dioxide using LaOCl-functionalized SnO2 nanowires for air-quality monitoring. Talanta, 2012, 88, 152-159.	5.5	77
103	Synthesis, characterization, and comparative gas-sensing properties of Fe2O3 prepared from Fe3O4 and Fe3O4-chitosan. Journal of Alloys and Compounds, 2012, 523, 120-126.	5.5	72
104	Detection of pathogenic microorganisms using biosensor based on multi-walled carbon nanotubes dispersed in DNA solution. Current Applied Physics, 2012, 12, 1553-1560.	2.4	27
105	Effective hydrogen gas nanosensor based on bead-like nanowires of platinum-decorated tin oxide. Sensors and Actuators B: Chemical, 2012, 173, 211-217.	7.8	26
106	Synthesis of single-crystal SnO2 nanowires for NOx gas sensors application. Ceramics International, 2012, 38, 6557-6563.	4.8	37
107	The quantum acoustomagnetoelectric field in a quantum well with a parabolic potential. Superlattices and Microstructures, 2012, 52, 921-930.	3.1	15
108	Giant enhancement of H2S gas response by decorating n-type SnO2 nanowires with p-type NiO nanoparticles. Applied Physics Letters, 2012, 101, .	3.3	48

#	Article	IF	CITATIONS
109	Design of SnO2/ZnO hierarchical nanostructures for enhanced ethanol gas-sensing performance. Sensors and Actuators B: Chemical, 2012, 174, 594-601.	7.8	174
110	A morphological control of tungsten oxide nanowires by thermal evaporation method for sub-ppm NO2 gas sensor application. Sensors and Actuators B: Chemical, 2012, 171-172, 760-768.	7.8	59
111	Electrochemical synthesis of polyaniline nanowires on Pt interdigitated microelectrode for room temperature NH3 gas sensor application. Current Applied Physics, 2012, 12, 1011-1016.	2.4	60
112	Gas sensor based on nanoporous hematite nanoparticles: Effect of synthesis pathways on morphology and gas sensing properties. Current Applied Physics, 2012, 12, 1355-1360.	2.4	42
113	Conducting polymer film-based immunosensors using carbon nanotube/antibodies doped polypyrrole. Applied Surface Science, 2011, 257, 9817-9824.	6.1	35
114	Systematic Study of the 4f Electronic State in RRhIn5 and RCu2Si2 (R: Rare Earth). E-Journal of Surface Science and Nanotechnology, 2011, 9, 446-453.	0.4	1
115	Preparing large-scale WO3 nanowire-like structure for high sensitivity NH3 gas sensor through a simple route. Current Applied Physics, 2011, 11, 657-661.	2.4	135
116	Electrochemical detection of short HIV sequences on chitosan/Fe3O4 nanoparticle based screen printed electrodes. Materials Science and Engineering C, 2011, 31, 477-485.	7.3	76
117	Gas sensing properties at room temperature of a quartz crystal microbalance coated with ZnO nanorods. Sensors and Actuators B: Chemical, 2011, 153, 188-193.	7.8	74
118	A comparative study on the NH <sub align="right">3 gas-sensing properties of ZnO, SnO<sub align=right>2, and WO_{3 nanowires. International Journal of Nanotechnology, 2011, 8, 174.}</sub </sub>	0.2	13
119	Novel silver nanoparticles: synthesis, properties and applications. International Journal of Nanotechnology, 2011, 8, 278.	0.2	26
120	On-chip fabrication of SnO2-nanowire gas sensor: The effect of growth time on sensor performance. Sensors and Actuators B: Chemical, 2010, 146, 361-367.	7.8	102
121	Synthesis of oleic acid-stabilized silver nanoparticles and analysis of their antibacterial activity. Materials Science and Engineering C, 2010, 30, 910-916.	7.3	103
122	Facile preparation of a DNA sensor for rapid herpes virus detection. Materials Science and Engineering C, 2010, 30, 1145-1150.	7.3	27
123	Highly reproducible synthesis of very large-scale tin oxide nanowires used for screen-printed gas sensor. Sensors and Actuators B: Chemical, 2010, 144, 425-431.	7.8	29
124	Gas-sensing properties of tin oxide doped with metal oxides and carbon nanotubes: A competitive sensor for ethanol and liquid petroleum gas. Sensors and Actuators B: Chemical, 2010, 144, 450-456.	7.8	110
125	Comparative study of gas sensor performance of SnO2 nanowires and their hierarchical nanostructures. Sensors and Actuators B: Chemical, 2010, 150, 112-119.	7.8	135
126	A facile thermal evaporation route for large-area synthesis of tin oxide nanowires: Characterizations and their use for liquid petroleum gas sensor. Current Applied Physics, 2010, 10, 636-641.	2.4	35

NGUYEN VAN HIEU

#	Article	IF	CITATIONS
127	DNA sensor development based on multi-wall carbon nanotubes for label-free influenza virus (type A) detection. Journal of Immunological Methods, 2009, 350, 118-124.	1.4	119
128	Thin film polypyrrole/SWCNTs nanocomposites-based NH3 sensor operated at room temperature. Sensors and Actuators B: Chemical, 2009, 140, 500-507.	7.8	99
129	Impact parameters on hybridization process in detecting influenza virus (type A) using conductimetric-based DNA sensor. Physica E: Low-Dimensional Systems and Nanostructures, 2009, 41, 1567-1571.	2.7	17
130	Facile synthesis of p-type semiconducting cupric oxide nanowires and their gas-sensing properties. Physica E: Low-Dimensional Systems and Nanostructures, 2009, 42, 146-149.	2.7	45
131	Highly sensitive thin film NH3 gas sensor operating at room temperature based on SnO2/MWCNTs composite. Sensors and Actuators B: Chemical, 2008, 129, 888-895.	7.8	204
132	Inclusion of SWCNTs in Nb/Pt co-doped TiO2 thin-film sensor for ethanol vapor detection. Physica E: Low-Dimensional Systems and Nanostructures, 2008, 40, 2950-2958.	2.7	34
133	Mixed SnO2/TiO2 included with carbon nanotubes for gas-sensing application. Physica E: Low-Dimensional Systems and Nanostructures, 2008, 41, 258-263.	2.7	67
134	Enhanced performance of SnO2 nanowires ethanol sensor by functionalizing with La2O3. Sensors and Actuators B: Chemical, 2008, 133, 228-234.	7.8	128
135	Low-temperature growth and ethanol-sensing characteristics of quasi-one-dimensional ZnO nanostructures. Physica B: Condensed Matter, 2008, 403, 50-56.	2.7	36
136	Unique Magnetic Properties of NdRhIn5, TbRhIn5, DyRhIn5, and HoRhIn5. Journal of the Physical Society of Japan, 2006, 75, 074708.	1.6	23
137	Fermi Surface and Magnetic Properties of PrTIn5 (T: Co, Rh, and Ir). Journal of the Physical Society of Japan, 2005, 74, 3320-3328.	1.6	13
138	Synthesis and Gas Sensing Properties of SnO ₂ Nanostructures by Thermal Evaporation. Advanced Materials Research, 0, 620, 350-355.	0.3	1